RAPID COMMUNICATIONS

PHYSICAL REVIEW B VOLUME 36, NUMBER 2 15 JULY 1987-I

Arsenic antisite defect As_{Ga} and $EL2$ in GaAs

B. K. Meyer, D. M. Hofmann, J. R. Niklas, and J.-M. Spaeth
Fachbereich Physik, University of Paderborn, Warburger Strasse 100A, 4790 Paderborn, Federal Republic of Germany
(Received 14 April 1987)

The microscopic structure of the paramagnetic anion antisite defect in semi-insulating GaAs was determined by optically detected electron-nuclear double resonance (ODENDOR). It is an arsenic-antisite–arsenic-interstitial (As_{Ga}-As_i) pair. It is shown, by optically detected ESR and ODENDOR experiments, that its energy levels and optical properties in the diamagnetic state are those of the $EL2$ defect.

The dominant midgap level $EL2$ in undoped GaAs is responsible for its semi-insulating properties. It is due to a defect of yet unknown microscopic structure, which has unique and fascinating properties. At low temperature it can be photoexcited into a metastable state which is responsible for the observed persistent quenching of the photocapacitance. It returns to the ground state only after thermal activation at 140 K.[1] ESR investigations of crystals grown under different melt stoichiometry conditions show that $EL2$ is related to an anion antisite (As_{Ga}) ESR signal.[2,3] Therefore, many defect models exist involving an anion antisite defect, isolated or combined with vacancies or an interstitial.[4–7]

The identification of $EL2$ with an As_{Ga}-As_i complex in Ref. 7 was based on a combination of ESR and deep-level transient spectroscopy measurements (DLTS) of electron-irradiated n-type GaAs. In the ESR experiments, however, only the hyperfine interaction with the central nucleus is resolved, whereas the hyperfine interactions and symmetry of the ligands cannot be deduced from the ESR spectrum. Therefore, the identification of $EL2$ in Ref. 7 was a very indirect one: the role of the As_i defect and the assignment of its charge state and position were based on theoretical predictions, a comparison of diffusion data, and speculations.

In this Rapid Communication we report on a direct experimental structure determination of the $EL2$ defect by optically detected electron-nuclear double-resonance (ODENDOR) experiments on the arsenic antisite defect in semi-insulating GaAs. A correlation between the energy levels and optical properties and the ESR and ENDOR spectra (i.e., its microscopic structure) is made by photoexcitation experiments in p-type GaAs. The $EL2$ defect is indeed an arsenic-antisite–arsenic-interstitial pair. From the ENDOR data the location and charge state of As_i can be inferred.

The ODENDOR signals are measured as radio-frequency- (rf) induced changes of the magnetic circular dichroism (MCD) under microwave resonance conditions.[8] Compared to our earlier ODENDOR investigations[9] the rf strength and the frequency range have been extended. The positions of the ENDOR lines were determined using digital filtering algorithms and an automatic peak-search program.[10] Undoped semi-insulating GaAs with an arsenic fraction in the melt of 0.5 ([As]/([As]+[Ga])) and semi-insulating GaAs:V yielded the same results.

Figure 1 shows the angular dependence of the ODENDOR lines in GaAs:V upon rotating the crystal in a (110) plane from $\mathbf{B}_0 \| [110]$ defined as 0° towards $\mathbf{B}_0 \| [100]$. The dots represent the ENDOR line positions, their size the line intensity. All lines are due to ^{75}As. The analysis of the angular dependence was complicated by several factors. For a tetrahedrally coordinated As antisite defect a simple angular pattern due to four ligands with [111] symmetry would be expected, two lines for $\mathbf{B}_0 \| [110]$ and one line for $\mathbf{B}_0 \| [100]$. A large quadrupole interaction

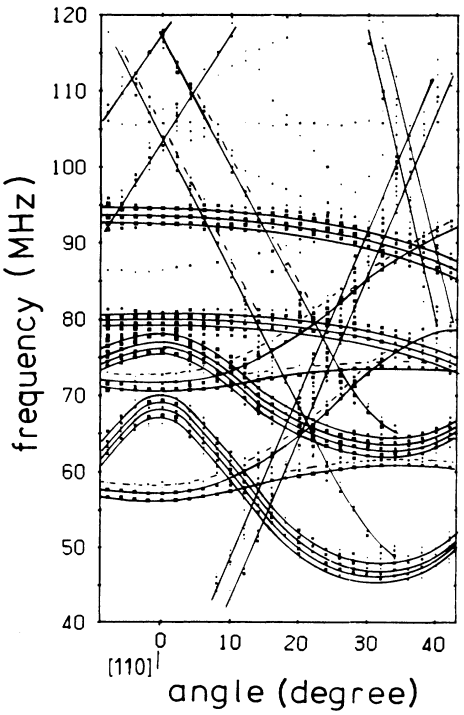

FIG. 1. Angular dependence of the ODENDOR lines of As_{Ga} in semi-insulating GaAs:V for rotation of the crystal in a (110) plane from [110] (0°) towards [100]. Solid lines and dashed drawn lines correspond to the four nearest As ligands, the dots above 80 MHz to the additional As interstitial nucleus.

(nuclear spin of ^{75}As $I=\frac{3}{2}$) influences the pattern so much that it is not recognized easily.[11] For each orientation of B_0 in a (110) plane one would expect 18 ENDOR lines due to four nearest neighbors (NN) of which two remain equivalent. There are many more lines due to additional splittings (see, e.g., around 80 and 95 MHz for $\mathbf{B}_0\|[110]$), which arise from a large pseudodipolar coupling of the nearest neighbors. The splittings are much larger than expected from current treatments of the effect,[12] due to a large anisotropic ligand-hyperfine (lhf) interaction.

Compared to our earlier ODENDOR experiments[9] on a GaAs:Cr sample the ENDOR lines were narrower by a factor of 2. Also the improved experimental conditions allowed us to extend the frequency range from about 90 to 300 MHz with a better resolution in order to distinguish whether a possible small distortion of the four nearest ligands or the pseudodipolar coupling effects were responsible for the splittings in the ENDOR angular dependence. This improvement in experimental conditions and crystal material was decisive. Our earlier interpretation that two types of antisite defects, an isolated defect and a distorted defect are simultaneously present in semi-insulating as-grown GaAs has to be revised. The additional lines attributed previously to distorted defects are due to the ENDOR lines of the four nearest As ligands split by pseudodipolar couplings. Similar effects were observed in the ENDOR pattern of the neutral gallium vacancy in GaP.[13]

The solid lines in Fig. 1 were calculated after diagonalizing the appropriate spin Hamiltonian[9] containing the central hf interaction and lhf and quadrupole interaction tensors for the [111] NN and the electron Zeeman term with the parameters given in Table I. The interaction tensors are axially symmetric with respect to the [111] axes within experimental accuracy. There are, however, two types of additional lines: (1) Satellite lines, indicated by dashed lines in Fig. 1, following the angular dependence of the nearest neighbors (solid lines). These are not explainable by indirect-coupling effects (see, however, the discussion of the quadrupole interaction below) and (2) ENDOR lines which do not follow the calculated angular dependence (see Fig. 1, the dots at frequencies above 80 MHz).

The full angular dependence of the additional lines above 80 MHz could not be followed in this crystal orientation, because it is hidden under the other strong lines. By measuring the ENDOR spectra for $\mathbf{B}_0\|[100]$ towards $\mathbf{B}_0\|[1\bar{1}0]$ in a (110) plane the variation of these lines in a frequency range from 100 to 140 MHz could be followed. Analysis yielded that they also belong to ^{75}As with [111] symmetry with interaction parameters given in Table I.

The additional ENDOR lines can be measured across the whole MCD spectrum and in all four ESR lines and thus belong to the same defect. The intensity of the ENDOR lines is lower by a factor 4–8 compared to the lines of the nearest ligands which indicates the presence of one single nucleus. This result is supported by a simulation of the ESR linewidth $W_{1/2}$ taking into account the measured lhf interactions including those of 12 As neighbors in a third shell, the ENDOR lines of which could be measured in a frequency range between 10–30 MHz (see below). Including one additional [111] As nucleus one obtains $W_{1/2,\mathrm{calc}}=32.5$ mT in excellent agreement with the experimental value of $W_{1/2,\mathrm{expt}}=33.5$ mT, whereas without As_i one calculates only 26 mT. Assuming instead four [111] nuclei on lattice sites (e.g., seventh As shell) $W_{1/2,\mathrm{calc}}$ would be 42 mT, thus far too large (spin-packet width taken from the ENDOR linewidth). Within the GaAs crystal structure one single [111] As ligand can only be an interstitial along [111]. Therefore, the positively charged $EL2$ defect is a As_{Ga}-As_i pair (Fig. 2) with C_{3v} symmetry. This symmetry is also clearly seen in the third-shell

TABLE I. Hyperfine and ligand hyperfine interaction parameters of the positively charged $EL2$ (As_{Ga}-As_i) defect. a and b are the isotropic and anisotropic lhf parameters, respectively; q is the quadrupole interaction constant. The interaction parameters for As IIIb nuclei could only be determined with less accuracy. They are very similar to those of shell IIIc.

	Interaction parameters		
	a (MHz)	b (MHz)	q (MHz)
Central As_{Ga} nucleus	2656 ± 15		
Ligand 1[a]	167.8	53.9 ± 0.1	12.2
Ligands 2–4	167.8 ± 0.1	53.9 ± 0.1	11.7 ± 0.1
Interstitial As_i	215 ± 2	44 ± 1	4.8 ± 0.2
As (IIIa)	35.2 ± 0.1	-1.3 ± 0.1	2.8 ± 0.1
As (IIIc)	19.5 ± 0.1	3.2 ± 0.1	0.9 ± 0.1

[a]From the experiment it is not possible to decide, whether ligand 1 has a slightly higher q value compared to ligands 2–4 or whether the isotropic interaction constant a is slightly larger.

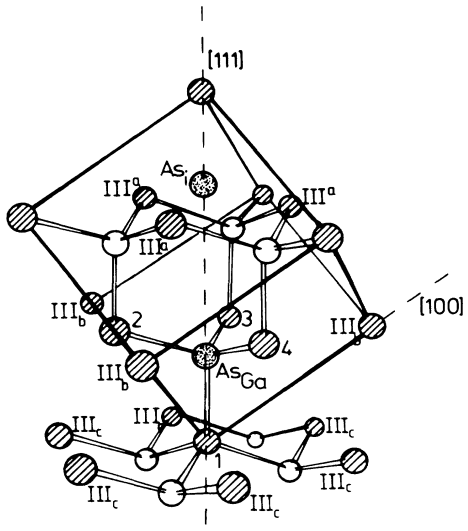

FIG. 2. Model of the As_{Ga}-As_i pair. The nearest As ligands are labeled 1 to 4. The 12 next nearest neighbors are labeled by III. Under the influence of the As_i they split into three subshells, labeled IIIa, IIIb, and IIIc. Hatched circles represent As, open circles Ga nuclei.

TABLE II. Influence of the charge state and place of the As interstitial on the quadrupole constant q of the four nearest As ligands [As(1)–As(4)]; q' denotes the deviation from axial symmetry and the angle θ the deviation of the tensor z axis from [111]. The experimental value of q for As(2)–As(4) is $|q| = 11.7 \pm 0.2$ MHz, $\theta = 0$, $q' = 0$. The value for As(1) can be 12.2 MHz. Since the shift of its ENDOR line from those of nuclei 2–4 is due to a combined effect of a and q, and a may also be changed slightly, q cannot be determined with more accuracy. $q = \frac{1}{2} Q_{zz}$, $q' = \frac{1}{2}(Q_{zz} - Q_{yy})$.

Site of As_i with respect to As_{Ga}	Ligand	Charge states As_i^- q (MHz)	q' (MHz)	θ (deg)	As_i^+ q (MHz)	q' (MHz)	θ (deg)	As_i^{3+} q (MHz)	q' (MHz)	θ (deg)
T_{d1}	As(1)	12.5	0	0	13.4	0	0	14.2	0	0
(2.44 Å)	As(2)–As(4)	13.3	2.9	−4	13.2	−1.7	5	15.6	−4	17
T_{d2}	As(1)	12.8	0	0	13.1	0	0	13.4	0	0
(4.88 Å)	As(2)–As(4)	13.3	0.8	−1	12.8	−0.6	1	12.3	2.1	2

(III) As ligands (12 nuclei). There are one subshell of six equivalent nuclei and two subshells of three equivalent nuclei each (see Fig. 2 and Table I).

The charge state of the interstitial must be such that its resulting electron spin is zero (i.e., As^+, As^-, As^{3+}). For a paramagnetic charge state, As_i^0, both constituents of the pair would be paramagnetic and could either have a fine-structure dipole-dipole interaction (estimated to be approximately 50 mT) or because of exchange interaction be in a spin-singlet or -triplet state. This is not consistent with the observed ESR spectrum.

The site of As_i is determined by estimating the ligand quadrupole interaction constants, which have two major contributions. One, $q(b)$, is due to the unpaired spin density in p orbitals at the ligands measured by the anisotropic lhf interaction, b,[14,15] and one, $q(p)$, is due to the electric field gradient caused by the charge distribution including the Sternheimer antishielding effect. The charge on As_{Ga}, As_i, and the ligands is estimated by analyzing their hyperfine data using a linear combination of atomic orbitals approach and equating spin density with charge density.[16] The measured hf and lhf data are compared to the values for the free As atom.[17] We find that 18% of the unpaired electron resides on As_{Ga}, 17% on each of the ligands 1–4, and 14% on the interstitial, while only 1% is on each of the 12 As neighbors in the third shell. The resulting total charge is 1.12 and was not normalized to 1. Including this in the total charge distribution according to which, e.g., the As_{Ga} has $+1.82e$, the NN $-0.17e$ etc. and treating the charges simply as point charges, one calculates for the neighbors 1 and 2–4, $q(p) = 6.3$ MHz and $q(b) = 6.7$ MHz; in total $q = 13$ MHz, in good agreement with $q_{expt} = 11.7$ MHz. For the additional As_i $q(b)$ is 5.4 MHz. The point-charge contribution for the nearest possible tetrahedral interstitial site is $q(p) = 6.4$ MHz; in total $q = 11.8$ MHz, which is too large compared to $q_{expt} = 4.8$ MHz. For the second tetrahedral interstitial site T_{d2} ($d = 4.88$ Å) the calculated q value is only 6.0 MHz, since $q(p)$ (proportional to $1/d^3$) amounts only to 0.6 MHz. This calculation gives a first evidence that As_i is located at a second nearest interstitial site.

The charge of the interstitial also influences the quadru-

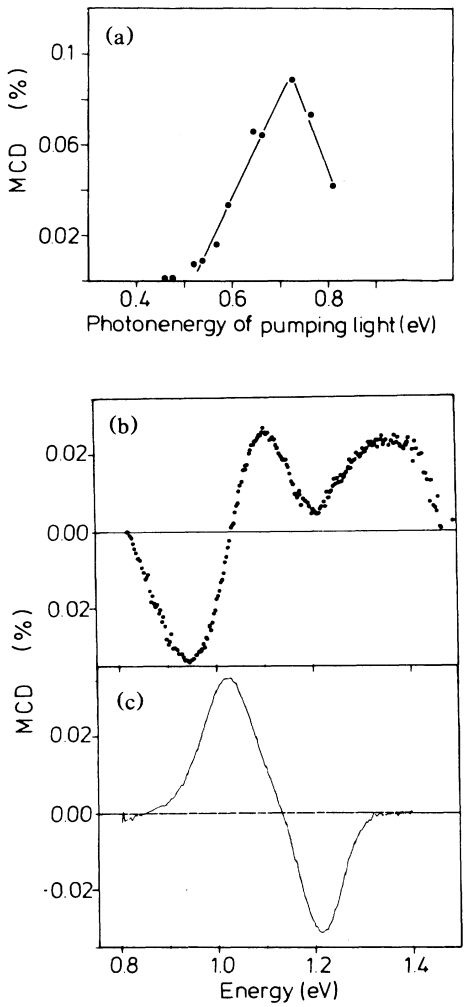

FIG. 3. (a) Excitation spectrum of the magnetic circular dichroism (MCD) of the As_{Ga}-As_i pair in p-type GaAs:Zn (photo-MCD). (b) MCD spectrum of the photo-excited As_{Ga}-As_i pair in p-type GaAs:Zn. (c) MCD spectrum of n-type GaAs:Si after 2 MeV electron irradiation 2×10^{17} e^-/cm^2.

pole interaction of the nearest ligands 1 and 2–4 (Table II). Estimating this also supports the T_{d2} site: on a T_{d1} interstitial site a charged interstitial would cause a large deviation from axial symmetry of the quadrupole tensors and a considerable deviation of the tensor z axes from a [111] direction described by the angle θ in Table II. This is not observed. Only the T_{d2} site of As_i^+ or As_i^- at 4.88 Å from As_{Ga} would be compatible with the experiment, since a small q' of 0.7 MHz could not be resolved within the ENDOR linewidth. The q values estimated for ligand 1 are slightly different from those for ligands 2–4 and may give rise to the dashed line in the ENDOR angular dependence of Fig. 1. Thus only three of the four NN's are equivalent [As(2)–As(4)].

The charged interstitial must also influence the As neighbors in the third shell. Three of the 12 nuclei see the charged As_i in the first neighbor distance ($d=2.44$ Å) (labeled as IIIa in Fig. 2). The As_i charge must cause a large quadrupole interaction on these three nuclei. The total q value of the IIIa nuclei is calculated to be 3.0 MHz assuming a positively charged As_i^+ and −4.5 MHz assuming a negatively charged As_i^-. Although the sign of q cannot be determined by the experiment, comparison shows that good agreement is achieved for the positively charged As_i (see Table I). This follows also from the compensation behavior of $EL2$. The influence of As_i on the q of nuclei in shells IIIb and IIIc is negligible.

We now address the question of whether the As_{Ga}-As_i complex can be identified with the $EL2$ defect. A correlation between the magnetic resonance spectra and the energy levels and optical bands can be made by performing optically detected ESR and ODENDOR measurements in p-type GaAs:Zn. In this material the Fermi level is at the Zn acceptor level, the defect +/++ level is empty. It can be populated by exciting electrons from the valence band into it. The MCD of the now populated state is monitored as a function of excitation photon energy [Fig. 3(a)]. Above a threshold of $E_v+0.52\pm0.02$ eV the MCD [Fig. 3(b)], ODESR and ODENDOR spectra of the As_{Ga}-As_i interstitial pair are observed. Above a second threshold $E_v+0.74\pm0.02$ eV the signal decreases again, since now a second electron is captured to form the diamagnetic pair. With the creation of this diamagnetic defect by pumping light ($h\nu>0.74$ eV), an absorption band at 1.2 eV appears, which shows the typical $EL2$ behavior, i.e., persistent bleaching and thermal recovery at 140 K.

Saturation of the conventionally detected ESR signal in as-grown undoped material has been reported.[18] Based on the analysis of the saturation behavior at low temperatures it is concluded[18] that ESR and ODESR detect the same antisite species, i.e., As_{Ga}-As_i. For plastically deformed and electron- or neutron-irradiated GaAs the spin-lattice relaxation time is orders of magnitudes shorter, although the ESR spectrum is identical to that in as-grown material.[19,20] Aggregation of $EL2$ defects produced in high local densities could cause this effect.

The presence of an additional isolated As_{Ga} in semi-insulating GaAs is excluded from our experiments. A possible candidate for an isolated antisite defect in GaAs is the defect produced by electron irradiation of n-type GaAs. It shows the identical central hyperfine splitting in its ESR spectrum; its MCD spectrum is, however, markedly different [see Fig. 3(c)]. Its shape, a single derivative, indicates an excited state only split by the spin-orbit interaction. It shows no metastable quenching properties; its MCD and ESR spectrum is not influenced by light irradiation. In semi-insulating GaAs only one defect, the As_{Ga}-As_i pair, is present with its typical MCD shape [Fig. 3(b)]. The ODESR and ODENDOR lines of As_{Ga}-As_i are connected only to this MCD.

In conclusion, the photoquenching properties and the energy levels of the As_{Ga}-As_i defect are identical to those of $EL2$.[21] We therefore conclude that $EL2$ is an As_{Ga}-As_i pair. The positively charged As_i is located at the second tetrahedral interstitial site. The isolated As_{Ga} cannot be identified with $EL2$.

[1]G. Vincent and D. Bois, Solid State Commun. **27**, 431 (1978).
[2]D. E. Holmes, K. R. Elliott, R. T. Chen, and C. G. Kirkpatrik, in *Semi-Insulating III-V Materials,* edited by S. Makram-Ebeid and B. Tuck (Shiva, Nantwich, 1982), p. 19.
[3]N. Tsukada, T. Kikuta, and K. Ishida, Jpn. J. Appl. Phys. **24**, L689 (1985).
[4]M. Kaminska, M. Skowronski, and W. Kuszko, Phys. Rev. Lett. **55**, 2204 (1985).
[5]J. Lagowski, H. C. Gatos, J. M. Parsey, K. Wada, M. Kaminska, and W. Walukiewicz, Appl. Phys. Lett. **40**, 342 (1982).
[6]J. A. Van Vechten, in *Microscopic Identification of Electron Defects in Semiconductors,* edited by N. M. Johnson, S. G. Bishop, and G. D. Watkins, Proceedings from the 1985 Materials Research Society Spring Meeting, Vol. 46 (Materials Research Society, Pittsburgh, 1985).
[7]H. J. von Bardeleben, D. Stievenard, and J. C. Bourgoin, Appl. Phys. Lett. **47**, 970 (1985).
[8]B. K. Meyer, J.-M. Spaeth, and M. Scheffler, Phys. Rev. Lett. **52**, 851 (1984).
[9]D. M. Hofmann, B. K. Meyer, F. Lohse, and J.-M. Spaeth, Phys. Rev. Lett. **53**, 1187 (1984).
[10]J. R. Niklas, Radiat. Eff. **72**, 39 (1983).
[11]J.-M. Spaeth, D. M. Hofmann, and B. K. Meyer, in Ref. 6, p. 185.
[12]T. E. Feuchtwang, Phys. Rev. **126**, 1628 (1962).
[13]J. Hage, J. R. Niklas, and J.-M. Spaeth, in *Defects in Semiconductors,* edited by H. J. von Bardeleben [Mater. Sci. Forum **10–12**, 259 (1986)].
[14]J. Owen and J. H. M. Thornley, Rep. Prog. Phys. **29**, 675 (1968).
[15]P. van Engelen, Phys. Rev. B **22**, 3144 (1980).
[16]U. Kaufmann and J. Schneider, in *Festkörperprobleme: Advances in Solid State Physics,* edited by J. Treusch (Vieweg, Braunschweig, 1980), Vol. 20, p. 87.
[17]J. R. Morton and K. F. Preston, J. Magn. Reson. **30**, 577 (1978).
[18]U. Kaufmann (private communication).
[19]R. B. Beall, R. C. Newman, and J. E. Whitehouse, J. Phys. C **19**, 3745 (1986).
[20]B. K. Meyer and J.-M. Spaeth, J. Phys. C **18**, L99 (1985).
[21]B. K. Meyer, D. M. Hofmann, and J.-M. Spaeth, J. Phys. C (to be published).